Journal of The Electrochemical Society, **146** (11) 4101-4104 (1999)
S0013-4651(99)05-034-X CCC: $7.00 © The Electrochemical Society, Inc.

In Situ Atomic Force Microscopy Imaging of Electrodeposition of Mixed Layers of Copper/Cuprous Oxide

A. Bonnefont,[a] R. Kostecki,[c,*] F. McLarnon,[c,*] J. C. Arrayet,[b] L. Servant,[b,*] and F. Argoul[a,*,z]

[a]*Centre de Recherche Paul Pascal, 33600 Pessac, France*
[b]*Laboratoire de Physico-Chimie Moléculaire, 33405 Talence Cedex, France*
[c]*Lawrence Berkeley National Laboratory, Berkeley, California 94720*

In situ atomic force microscopy (AFM) was applied to the dynamic characterization of the growth of mixed Cu/Cu_2O layers obtained by galvanostatic electrodeposition from alkaline Cu(II) lactate solutions. The correlation of the cathode potential profile with the average topographic profiles computed from the AFM images provided evidence for two transitions in the deposit growth during which the average growth velocity underwent rapid accelerations, the first one corresponding to zero interfacial concentration (Sand's time) and the second one to the emergence of the oscillations by a smooth transition. Despite its temporal resolution, the AFM technique could not capture the details of a single oscillation, but it proved to be quite adequate for tracking the general evolution of the electrode surface.

Manuscript submitted May 10, 1999; revised manuscript received June 21, 1999.

Electrochemical systems are generally more complex than homogeneous chemical systems because they involve both electrokinetic and chemical processes, and they are also noted for their ability to undergo complex nonlinear dynamic processes such as oscillations. Oscillatory dynamics are quite common in electrochemical systems; they have been observed in electrodissolution, electrocatalytic reactions, and cathodic processes.[1,2] Although oscillatory dynamics are less common in electrodeposition experiments, they have been encountered on differents metals.[2,3] Copper electrodeposition is one of the most studied systems.[4-6] It has been recently reported by Switzer *et al*.[6-9] that layered Cu nanostructures could be electrodeposited from aqueous solutions with fixed current, concomitant with oscillatory dynamics of the cathode potential. These self-assembled films were deposited from a stirred solution of 0.6 M $CuSO_4$ and 3.0 M lactate (at 30°C) on Pt electrodes, and potential oscillations were observed within the pH range 8.5-10. In a very recent publication[6,9] these temporal modulations of the electrodeposition process were studied it *in situ* by weighing the as-deposited film with an electrochemical quartz crystal microbalance (EQCM). The close correspondence of the temporal evolution of the EQCM frequency shift with the potential oscillations is an unambiguous demonstration of the pulsating nature of the electrodeposition process in this system.

In particular, Switzer *et al*.[6-9] report that the period of these oscillations is not influenced by the current density in the range from 0.1 to 2.25 mA/cm^2, whereas the composition of the layered structure depends on the current density. Moreover, they also showed that both the period of these oscillations and the composition of the deposit are very sensitive to the solution pH. The composition of the modulated phase is periodic, including layers of a mixture of Cu_2O and Cu (a few tens of nanometers thick) and thin layers of pure Cu_2O (a fraction to a few nanometers). Despite the recent characterization of these complex behaviors by Switzer *et al*.,[6,8,9] many questions remain unanswered on the exact origin of these oscillations and on the physical mechanisms which are involved in determining the temporal and the spatial periodicity of the layered structure. From these published studies, one would be tempted to conclude that the temporal period of the voltage oscillations is independent of both the spatial modulation of the nanostructured Cu/Cu_2O layers and their compositions (see Table I of Ref. 8).

To provide possible answers to these questions, we performed simultaneous atomic force microscopy (AFM) and chronopotentiometric measurements on the Cu/lactate electrodeposition system. This note is a preliminary report of our investigations. Keeping in mind that this system can exhibit different spatial and temporal scales, our discussion aims at showing that the electrodeposition process undergoes successive stages and that these stages are reflected in the growth velocity. We show that the AFM technique is quite efficient for probing *in situ* the average dynamics of the growth process, and that it may be also used to capture the dynamics of the oscillations within a very small area of the electrode surface.

Experimental

The working electrode (cathode) was made of a Cu foil which was first polished mechanically (wet sandings down to a grit size of 1 μm) and then electropolished in H_3PO_4 (72.5%) with an anodic current of 100 mA cm^{-2} for 5 min. The surface of the cathode in contact with the electrolyte was a disk with an area of 1.24 cm^2. The volume of solution above the cathode was about 0.25 mL. A counter electrode was made with a thin (~500 μm) hemicylinder Pt wire and the entire setup was immersed in a $CuSO_4$/lactate solution and con-

Table I. Computed values of the growth v_z and scanning *vs.* tanα velocities along the *Z* direction, as extracted from the analysis of Fig. 4 using Eq. 4 and 5.

Snapshot	$d<h>/dt$	v_z (Å s^{-1})	$\bar{\Delta}$ (Å s^{-1})
a	−3.3		
		5.6	18
b	14.5		
		4.3	20.5
c	−5.9		
		3.3	18.5
d	−12.6		
		3.6	18
e	−5.4		
		2	14.8
f	9.4		
		1.5	15.8
g	−6.4		
		4.05	20.9
h	14.5		
		4.4	20.26
i	−5.76		
		2.2	15.86
j	10.1		
		0.6	19
k	−8.9		
		0.7	19.16
l	10.26		

* Electrochemical Society Active Member.
z E-mail: argoul@crpp.u-bordeaux.fr

S0013-4651(99)05-034-X CCC: $7.00

nected to a EG&G Princeton Applied Research, model 362 galvanostat/potentiostat. To prepare the solution (0.04 mol L^{-1} Cu(II) and 3.5 mol L^{-1} lactate), 1 g of Cu(II) sulfate pentahydrate was added to 25 mL of 85% lactic acid under vigourous stirring. The solution pH was then made alkaline by the successive addition of increments (10 mL) of 5 mol L^{-1} NaOH over a period of a few minutes (the total volume of added NaOH was 60 mL). This solution was then stirred overnight. Finally, its pH was adjusted to 9.0 by the addition of a few drops of 98% H_2SO_4 and the solution was completed by water to make 1 L. A Cu wire was used as a quasi-reference electrode. The experiments were performed in the galvanostatic mode and for the example illustrated in this article, the current density was fixed to $j = 0.125$ mA cm^{-2}. The cathode potential with respect to the reference electrode was acquired every 1 s with a DAS20 by Keithley/Metrabyte data acquisition board.

The electrochemical cell was placed in a Molecular Imaging scanning probe microscope coupled with a Park Scientific Instruments electronic controller. The AFM images were recorded in the constant-force mode, *i.e.*, the piezoelectric scanner followed the surface profile of the sample and it adjusted itself to the changing profile of the surface. The typical radius of curvature of the tip end (silicon nitride) was 500 Å. Surface morphology changes were monitored simultaneously with Cu cathode potential with respect to the reference electrode. In the following all potentials are quoted with respect to the Cu reference electrode.

As depicted in Fig. 1a, during the recording of an AFM image, the tip moved along the X-axis (scan direction) and the Y-axis (sweep direction): after each line was swept in the *Y* direction, the tip moved along *X* to the next line. The direction of the movement along *X* is constant during one scan [for example, from D (down) to U (up) as drawn in Fig. 1], and it changes its direction at the next scan (from U to D). Therefore, the beginning of each AFM image, as time increases, is alternatively located at U and at D. A probable small tilt of the electrode surface prior to the beginning of the experiment, with respect to the laboratory frame, must be considered, because it can interfere with the estimation of the interface velocity during deposit growth. In Fig. 1b and c, we illustrate the influence of an initial tilt angle α of the electrode surface along the scan direction (X) upon the effective measurement of vertical displacement of the growing surface.

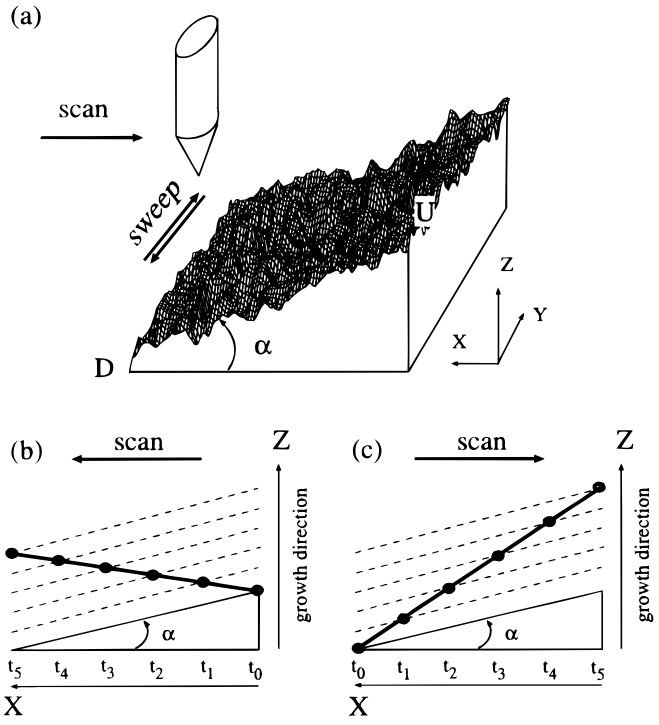

Figure 1. (a) Schematic diagram of AFM scanning of the copper cathode surface: the growth takes place along the *Z*-axis, the tip, parallel to the Z-axis, is swept line by line parallel to the *Y*-axis, and it scans alternatively from D to U along the *X*-axis; (b) and (c): projection of the copper electrode in the (*X*, *Z*) plane for two scan directions of the tip (along $X > 0$ for b, along $X < 0$ for c), the dashed line represents the projection in the (*X*, *Z*) plane of the growing cathode surface at various sampling times t_i, assuming a constant growth velocity. The time t_i is proportional to the time required for a line to be swept along the *Y*-axis by the tip. In b the tip is initially located at U and it moves toward D ($X > 0$) whereas in c it is initially located at D and moves toward U ($X < 0$).

Results

We report in Fig. 2 a set of AFM images of the Cu electrode, recorded in the galvanostatic mode ($j = 0.125$ mA/cm^2).The successive images show clearly that a grain-like structure of the surface appears to grow uniformly on panel b. The scan direction is indicated by the white arrows. The topography exhibits a morphological change, especially with respect to the grain shape, between images f and g, concurrent with the beginning of the oscillations. As time increases, the grain morphology does not evolve so rapidly with time, as was the case for panels a to f. Each image represents a surface of 1 μm^2. The corresponding cathode potential is displayed in Fig. 3. The dashed vertical lines in Fig. 3 indicate the time when each image recording began with respect to the labeling of Fig. 2.

In order to provide deeper insight into the growth process, we show in Fig. 4 for each AFM image of Fig. 2, the averaged value $\langle h(X, Y)\rangle_Y$ of the AFM signal along each sweep line (*Y*-axis), as a function of time, together with the corresponding cathode potential. Assuming that the growth takes place perpendicular to the surface at

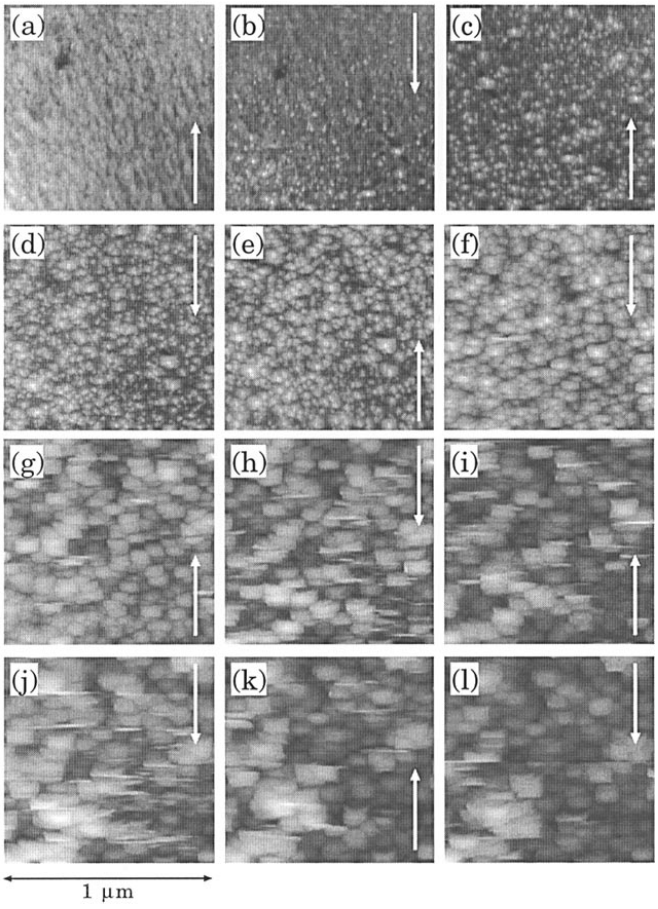

Figure 2. AFM images of the copper electrode as a function of time. Each panel is obtained for alternate scan directions (see text) and each image requires 51.2 s to be recorded. White arrows show the direction of the scan.

S0013-4651(99)05-034-X CCC: $7.00

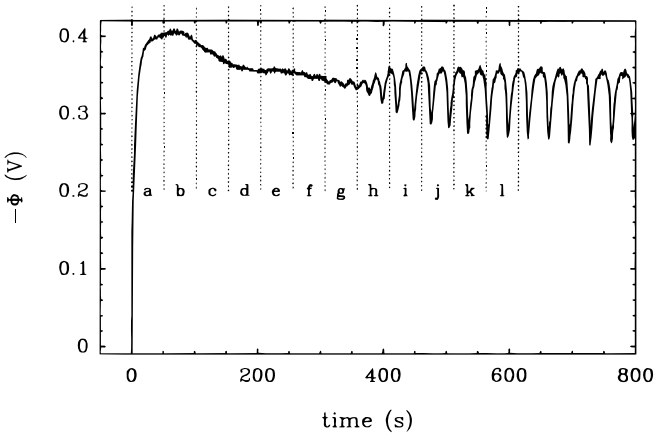

Figure 3. Signal of the cathode potential Φ (recorded *vs.* a Cu reference electrode) showing the emergence of periodic oscillations after an induction period of about 300 s.

a constant velocity, this averaged signal probes the evolution of the thickness of the deposit, and appears, as seen in Fig. 4, roughly as a monotonic function of time during the recording of one AFM image. Note that the slopes (reported in Å s^{-1} below each AFM data set on Fig. 4) of these curves alternate in sign between successive scans. The error bars which are also reported in these plots represent the mean dispersion $\sigma = \sqrt{<(h - <h>_Y)^2>_Y}$, of the AFM signal computed along each sweep line (Y) with respect to its average. Therefore this dispersion expresses the roughness of the surface.

Regarding Fig. 1b and c which correspond to a projection of Fig. 1a in the (X, Z) plane, these plots illustrate the coupling of the tip displacement with the surface growth during a single scan. The electrode surface position is represented by its projection (dashed segments) along the (X, Z) plane for successive times t_0 to t_5. The distance between each line corresponds to the vertical growth of the electrode surface during the time interval $t_{i+1} - t_i$ chosen here as constant. In our representation, we assume as a first approximation that the growth velocity of the interface along Z is constant. In this simplified model where the surface is assumed to be unroughened, the average height $<h>_Y$ measured by the AFM tip at each time t_i is reported as filled circles. When the growth velocity is constant (as illustrated in Fig. 1b and c), these points can be connected by a straight line. The slope of this line corresponds to the effective average displacement of the AFM tip along Z.

If we define v_z as the vertical velocity of the growing electrode with respect to the laboratory frame, v_s the scanning velocity and α the tilt angle of the surface, the vertical velocity (averaged along Y) of the AFM tip during the time interval dt reads

$$\frac{d<h>(t)_Y}{dt} = v_z + \epsilon v_s \tan\alpha \qquad [1]$$

where $\epsilon v_s \tan\alpha$ is the component of the velocity of the tip during the scan due the initial tilting of the electrode surface ($\epsilon = +1$) if the tip moves from U to D, ($\epsilon = -1$) on the opposite scan direction. This equation shows that the velocity $d<h>_Y/dt$ should be independent of time during a single scan if the electrodeposited layer growth speed v_z is constant, and that this slope changes by the quantity 2 tan αv_s between successive scans. The slope $d<h>_Y/dt$ of the curves $<h>(t)$ should be greater when $\epsilon = +1$ (scanning from U to D) than when $\epsilon = -1$ (scanning from D to U), the scanning velocity v_s being constant. This is indeed what is generally observed in Fig. 4.

More precisely, the alternate linear dependence of $d<h>_Y/dt$ as a function of time is evidenced on Fig. 4a to l. We note from images g to l that although the sign alternation is preserved, the average $<h>_Y(t)$ signal is no longer strictly linear during each scan and its mean dispersion (accounted by the error bars) increases with time, which demonstrates a roughening of the deposit interface with respect to panels a to g.

Assuming that the growth velocity is constant during one scan, one can extract from each AFM image a numerical value for $d<h>_Y/dt$

$$\left(\frac{d<h>_Y}{dt}\right)_{(i)} = v_z + v_s \tan\alpha \quad (\epsilon = +1) \qquad [2]$$

$$\left(\frac{d<h>_Y}{dt}\right)_{(i+1)} = v_z - v_s \tan\alpha \quad (\epsilon = -1) \qquad [3]$$

Summing the above equations we obtain an estimate of v_z, averaged over two successive images

$$v_z = \frac{1}{2}\left\{\left(\frac{d<h>_Y}{dt}\right)_{(i)} + \left(\frac{d<h>_Y}{dt}\right)_{(i+1)}\right\} \qquad [4]$$

Note that the difference between Eq. 2 and 3 should remain constant if we assume the tilt angle is constant

$$v_s \tan\alpha = \frac{1}{2}\left\{\left(\frac{d<h>_Y}{dt}\right)_{(i)} - \left(\frac{d<h>_Y}{dt}\right)_{(i+1)}\right\} \qquad [5]$$

Using Eq. 4 and 5, we report in Table I the values computed from the set of images shown in Fig. 2. The difference $\Delta = d<h>_Y/dt\}_{(i)} - d<h>_Y/dt_{(i+1)}$ appears, although not strictly constant, to be homogeneously distributed around an average value $\Delta \sim 18$ Å s^{-1}. This evidence supports the assumption that the initial tilt angle is preserved during the growth process (v_s being constant).

A striking piece of evidence shown by Table I is that the growth velocity is a maximum for images a-b and g-h. Moreover, for images a-b, the maximum velocity is concurrent with the maximum of the electrode potential which appears at Sand's time,[10] when the electrode becomes depleted in Cu(II) reducible species. Images g-h correspond to the emergence of the oscillations and Table I shows that an increase of the growth velocity also occurs at that time, at the end of a slowing-down phase of the growth. Beyond image i of Fig. 2, the growth velocity decreases, and the Cu/cupric lactate system presumably reaches a pseudostationary growth regime.

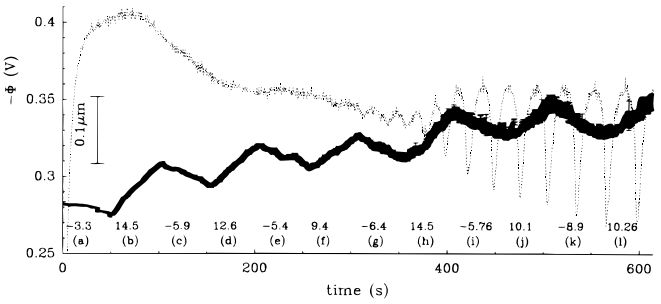

Figure 4. Comparison of the signal of the cathode potential Φ (dotted line) with the temporal evolution of the averaged electrode height, as deduced from AFM experiments (over the Y-axis) and its dispersion (errors bars). Each segment of $<h>_Y$ is labeled with the same letter as in Fig. 2 for the sake of clarity of the figure. The numbers reported below the plot of $<h>_Y(t)$ at the beginning of each scan (AFM image) correspond to the slopes $d<h>_Y/dt$ (in Å s^{-1}) evaluated for each scan. The different signs of these slopes are due both to the initial tilt of the surface and to the alternate scan directions from one image to the next one, as depicted in Fig. 1.

Discussion and Conclusion

This paper has presented an effort to probe *in situ* the electrodeposition of mixed copper/cuprous oxide from lactate solutions, using AFM. Our results suggest that the induction time period, which is observed prior to the settling of the potential oscillations, plays a crucial role in the growth mechanism. During that period, the topography of the electrode changes significantly. In an attempt to explain our results, we suggested the use of a simple model assuming constant growth velocity along the vertical direction. This analysis pro-

S0013-4651(99)05-034-X CCC: $7.00

vided evidence for significant changes of the growth speed, first at the end of the induction time (prior to Sand's time) and second when the oscillations emerged. In the intermediate regime (after Sand's time and prior to the oscillations) the reduction of solvent species and a local increase of the pH could change the copper cation complexes from lactate to mixed complexes with hydroxide and lactate anions, whose reduction to cuprous oxide could then be favored. We could not, in this preliminary experiment, correlate the potential oscillations with a temporal modification of the growth velocity, but we think that this could be done by reducing the AFM scan to a smaller portion of the electrode and increasing the sweep rate. This work is currently in progress.

This AFM study provides direct measurement of the average growth velocity v_z at different stages of the electrodeposition process, and these data are reported in Table I. One would be tempted to compare these values with a direct computation of the growth velocity deduced from the mass conservation equation at the interface

$$\rho_{dep} v_z = -\frac{j}{2F} M_{dep} \qquad [6]$$

where dep represents either Cu or Cu_2O, j is the current density, ρ is the density of the deposit (g cm^{-3}), M is the molar mass of deposited material (Cu or Cu_2O), and F is the Faraday constant. One may evaluate an order or magnitude of v_z by considering a compact deposition of Cu or Cu_2O whose densities are, respectively, 8.94 and 6.10 g cm^{-3}. With $j = 0.125$ mA cm^{-2}, one obtains $v_z = 0.46$ Å/s for pure compact copper deposition and $v_z = 1.52$ Å/s for pure compact cuprous oxide deposition. These values compare well with the above measured values of v_z (see Table I). Note that the experimental values of v_z obtained by our AFM study are significantly higher than these predictions in the induction stage of the growth process and at the initiation of the oscillations. These differences may originate from an enhancement of the deposit porosity resulting in a smaller apparent density of Cu (or Cu_2O) and inducing therefore, an increase of the v_z. This conclusion is well supported in images g and h and by the increase of the dispersion in $< h >_Y (t)$ as represented by the error bars in Fig. 4. However, this porosity enhancement is not strictly reflected in the dispersion of $< h >_Y (t)$ on panels b and c of this figure. This effect could be explained by the finite size of the AFM tip (500 Å radius of curvature) although a tip of 500 Å radius of curvature certainly can and does detect particles much smaller than 500 Å. The observed high average growth velocity at different stages of the electrodeposition process may also be partially explained by the loose structure of the growing film material, a large number of point defects, hydration, electrolyte enclosure. We also note that when the oscillations are established (after panel j of Fig. 4) the velocity of the growth appears as intermediate between those estimated for pure compact copper and pure compact cuprous oxide. This observation supports the composite layered structures evidenced in previous publications.[6-9]

Finally, to compare the composition of our deposits with previous studies, we performed *ex situ* Auger analysis of the deposits. Our first analysis shows that during the oscillations we obtain a composite film of Cu and Cu_2O, which is consistent with our previous discussion. Nevertheless, we failed to confirm by Auger the modulated structures reported by Switzer *et al.*[6-9] by different techniques. This limitation could be explained by a greater porosity of our deposits, or it could be due to a different growth mechanism because our experimental conditions are slightly different from theirs.

Acknowledgments

We are very grateful to F. Kong for his help in the design of the experiment and his technical support. We also thank J. F. Muzy and A. Arneodo for stimulating and fruitful discussions on the image analysis. This work was supported by the France-Berkeley fund. A.B. was partly funded by the Centre National d'Etudes Spatiales (CNES) under contract 97/151077300.

References

1. J. Wojtowicz, *Modern Aspects of Electrochemistry*, Vol. 8, p. 47, Butterworths, London (1972).
2. J.-L. Hudson and T.-T. Tsotisis, *Chem. Eng. Sci*, **49,** 1493 (1993).
3. F. Argoul and A. Kuhn, *J. Electroanal. Chem.*, **359,** 81 (1993).
4. F.-W. Schlitter, G. Eichkorn, and H. Fischer, *Electrochim. Acta*, **13,** 2063 (1968).
5. H. Jehring and U. Kuerschner, *J. Electroanal. Chem.*, **75,** 799 (1977).
6. J.-A. Switzer, C.-J. Hung, L.-Y. Huang, F.-S. Miller, Y. Zhou, E.-R. Raub, M. Shumsky, and E. Bohannan, *J. Mater. Res.*, **13,** 909 (1998).
7. J.-A. Switzer, C.-J. Hung, L.-Y. Huang, E.-R. Switzer, D.-R. Kammler, T.-D. Golden, and E.-W. Bohannan, *J. Am. Chem. Soc.*, **120,** 3530 (1998).
8. E.-W. Bohannan, L.-Y. Huang, F.-S. Miller, M.-G. Shumsky, and J.-A. Switzer, *Langmuir*, **15,** 813 (1999).
9. J.-A. Switzer, B.-M. Maune, E.-R. Raub, and E.-W. Bohannan, *J. Phys. Chem., B*, **103,** 395 (1999).
10. A.-J. Bard and L.-R. Faulkner, *Electrochemical methods, Fundamentals and Applications*, John Wiley & Sons, New York (1980).